

Towards Trustworthy Wi-Fi Sensing: Systematic Evaluation of Deep Learning Model Robustness to Adversarial Attacks

Shreevanth Krishnaa Gopalakrishnan* and Stephen Hailes

Department of Computer Science
University College London

{shreevanth.gopalakrishnan, s.hailes}@ucl.ac.uk

Abstract

Machine learning has become integral to Channel State Information (CSI)-based human sensing systems and is expected to power applications such as device-free activity recognition and identity detection in future cellular and Wi-Fi generations. However, these systems rely on models whose decisions can be subtly perturbed, raising concerns for security and reliability in ubiquitous sensing. Quantifying and understanding the robustness of such models, defined as their ability to maintain accurate predictions under adversarial perturbations, is therefore critical before wireless sensing can be safely deployed in real-world environments.

This work presents a systematic evaluation of the robustness of CSI deep learning models under diverse threat models (white-box, black-box/transfer, and universal perturbations) and varying degrees of attack realism. We establish a framework to compare compact temporal autoencoder models with larger deep architectures across three public datasets, quantifying how model scale, training regime, and physical constraints influence robustness. Our experiments show that smaller models, while efficient and equally performant on clean data, are markedly less robust. We further confirm that physically realizable signal-space perturbations, designed to be feasible in real wireless channels, significantly reduce attack success compared to unconstrained feature-space attacks. Adversarial training mitigates these vulnerabilities, improving mean robust accuracy with only moderate degradation in clean performance across both model classes. As wireless sensing advances towards reliable, cross-domain operation, these findings provide quantitative baselines for robustness estimation and inform design principles for secure and trustworthy human-centered sensing systems.

Keywords: WiFi sensing, Channel State Information (CSI), robustness evaluation, adversarial attacks, adversarial training, human activity recognition, gait identification, benchmarking

1 Introduction

Traditionally, sensing and localization using wireless communication signals were considered supplementary functionalities supporting the services of cellular and Wi-Fi networks. However, with the growing demand for intelligent environments – ranging from homes and offices to airports and care facilities – the number of use cases that depend on accurate positioning, detection, and recognition of humans has increased dramatically. Historically, communication and sensing relied on dedicated waveforms and protocols, but these boundaries have blurred significantly in recent years.

At a system level, the core requirements for indoor sensing can be distilled into *accuracy, privacy, security, and availability*. Accuracy remains the primary goal of technology development. Privacy concerns enforcing strict data-protection standards and preventing unauthorized access to sensing outputs, ensuring that sensing does not capture or reconstruct a user’s likeness without consent. Security, by contrast, denotes the system’s ability to withstand malicious interference or intentional manipulation. Availability refers to maintaining reliable operation whenever needed. System *integrity* then emerges from the interplay of security and accuracy. For detailed taxonomies of other sensing modalities, we refer the reader to [1].

Among the emerging technologies, Channel State Information (CSI)-based wireless sensing has proven particularly promising. It enables device-free, fine-grained, and partially privacy-preserving human sensing using commodity Wi-Fi devices. CSI captures multipath channel characteristics that can be leveraged for human activity recognition (HAR), localization, and identification, offering high-resolution perception. Early Wi-Fi sensing was enabled by Halperin et al.’s Intel 5300 CSI Tool [2], which exposed per-subcarrier channel data but required modified drivers and offline processing. However, recent toolchains and platforms such as Atheros [3], Nexmon [4], ESP32 [5], and ZTECSITool [6], have since enabled real-time, low-cost, and portable CSI-based wireless sensing without specialized hardware.

Key Research Issues

Machine Learning (ML) has become central to CSI-based sensing, mapping temporal and spectral channel variations to human-centric tasks. Yet, these models are inherently vulnerable to small, carefully crafted input modifications – adversarial perturbations – that exploit the fragility of their learned decision boundaries. In CSI settings, this challenge is further compounded by time-domain operation and strict physical-layer constraints, which make both constructing and defending against such perturbations fundamentally dif-

*Corresponding author

ferent from well-studied computer vision cases [7].

Existing work has explored threats at the physical and network layers, but the underlying goal of integrity attacks is consistent: to drive the ML model toward incorrect decisions by manipulating its inputs. Thus, regardless of where an attack is launched, the central vulnerability resides within the models. As a result, effective defense must begin with a systematic understanding of how CSI-based classifiers behave under diverse adversarial conditions.

Despite the growing number of CSI datasets and architectures, there is a lack of a systematic evaluation of model robustness. Prior works such as WiAdv [8], WiIntruder [9], and SecureSense [10] have demonstrated that adversarial perturbations can degrade HAR performance, yet they differ widely in experimental setup, model scale, and attack assumptions. Moreover, few studies incorporate *physically meaningful constraints*, such as channel correlation, Doppler coherence, which determine whether perturbations are realizable in real wireless environments. These limitations motivate a unified robustness evaluation framework for CSI-based sensing.

Comparison with the State of the Art

Several surveys and technical papers provide detailed overviews of CSI-based sensing, tracing its evolution from Received Signal Strength Indicator (RSSI)-based methods and highlighting its potential societal applications in alignment with future Wi-Fi and cellular generations. Most of these works focus on performance under benign conditions [11, 12, 13, 14, 15, 16, 17, 18]. Complementary studies aim to improve raw accuracy and generalization through refined processing pipelines, environment-independent representations, or cross-domain adaptation [19, 20, 21, 22, 23, 24, 25]. More recently, robustness-oriented research has explored the effects of signal injections, universal perturbations, and adversarial training [26, 10, 8, 27, 28, 29]. However, these efforts are often confined to specific models or attack families and lack standardized evaluations.

This paper fills these gaps by presenting a comprehensive evaluation of CSI-based deep learning model robustness under diverse threat models, spanning multiple datasets, architectures, and training paradigms, and incorporating unconstrained and physically realistic perturbations within a unified experimental framework.

Summary of Novel Contributions

This work provides the first systematic evaluation of ML adversarial robustness for CSI-based human sensing under realistic wireless constraints. We envisage that this line of research will yield practical insights for building secure and trustworthy Wi-Fi sensing systems. To this end, we:

1. Benchmark white-box, black-box, and universal adversarial attacks across diverse CSI datasets for sensing tasks like activity recognition and gait-based human identification.
2. Quantify how model scale and architecture influence robustness, comparing lightweight temporal autoencoder-based models with larger deep networks.

3. Introduce physically constrained perturbations that preserve spectral, spatial, and temporal correlation, providing more realistic attack baselines.
4. Evaluate the effectiveness of adversarial training as a defense mechanism, balancing clean accuracy and robustness.
5. Release a modular open-source framework for use with other datasets, models, attacks & defenses.

2 Background

This section provides an overview of how Wi-Fi signals can be repurposed for device-free sensing and human activity recognition, tracing the evolution from classical signal strength- and radar-based methods to fine-grained CSI sensing. It further introduces the emerging security and privacy challenges, culminating in recent efforts to characterize and defend against adversarial attacks on time-series models in this domain.

2.1 WLAN-based sensing

Wireless Local Area Network (WLAN)-based sensing has gained significant attention as it enables localization and activity recognition using existing Wi-Fi infrastructure. Three main approaches exist: Received Signal Strength Indicator (RSSI or RSS), Passive Wi-Fi Radar (PWR), and Channel State Information (CSI)-based sensing (SENS) [30]. All are based on the principle that environmental dynamics alter wireless propagation through multipath effects, frequency shifts, and attenuation.

RSS is coarse-grained, susceptible to multipath fading even in static environments, and challenging to use in robust detectors. PWR, inspired by bistatic radar, extracts parameters such as Angle of Arrival (AoA), Time of Flight (ToF), Time Difference of Arrival (TDoA), and Doppler Frequency Shift (DFS). Despite algorithmic maturity, PWR faces physical constraints: a 2.4 GHz Wi-Fi channel with 20 MHz bandwidth offers insufficient ToF resolution for fine-grained indoor sensing; self-interference also remains a limitation [31]. CSI differs by exploiting the fine-grained information embedded in the wireless channel. It provides the highest fidelity but is also highly sensitive to environmental variations [16].

The IEEE 802.11 family defines Wi-Fi standards for WLAN technologies [32]. While Wi-Fi sensing has been explored for over a decade, earlier standards did not explicitly support it. The recent IEEE 802.11bf amendment introduces a landmark change: Wi-Fi is now formalized as a joint communication and sensing technology. 802.11bf specifies new PHY and MAC layer mechanisms to enable standardized sensing measurements, facilitating interoperability across devices. This shift will allow developers to build cross-platform sensing applications for localization, activity recognition, and environment monitoring. Its impact, however, will depend on adoption by chipset vendors and manufacturers [33].

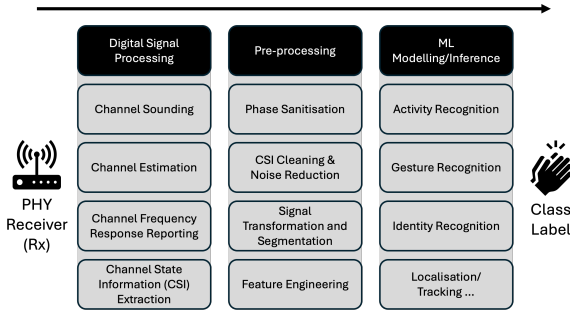


Figure 1: CSI processing pipeline – from signal reception to classification result

2.2 Channel State Information (CSI)

In an Orthogonal Frequency Division Multiplexing (OFDM)-based Wi-Fi system, the channel between transmitter and receiver can be represented as a three-dimensional CSI tensor:

$$H \in \mathbb{C}^{N_r \times N_t \times K} \quad (1)$$

where N_r and N_t denote the number of receive and transmit antennas, and K is the number of subcarriers. Each entry is a complex coefficient capturing amplitude attenuation $|H|$ and phase shift $\angle H$ for subcarrier k on the (i, j) antenna link:

$$H_{i,j}(k) = |H_{i,j}(k)| e^{j\angle H_{i,j}(k)} \quad (2)$$

CSI is typically sampled at high rates (1–10 kHz), forming time-series that encode variations in the propagation channel. Human presence, gestures, and activities leave distinctive temporal and spatial signatures in the CSI amplitude and phase. Since these patterns are not directly interpretable, machine learning methods are employed for tasks such as presence detection, fall detection, and activity recognition.

The end-to-end CSI processing pipeline, visualized in Figure 1, begins at the *physical (PHY) layer*, where transmitted Wi-Fi packets are received by one or more antennas and the channel is estimated using pilot symbols embedded in each orthogonal frequency-division multiplexing (OFDM) frame. The receiver computes the Channel Frequency Response (CFR) across all subcarriers and antennas, yielding complex CSI coefficients that capture amplitude attenuation and phase shift caused by multipath propagation. These raw CSI measurements are then passed through a sequence of *pre-processing* operations such as phase sanitization, denoising, filtering, and normalization to remove hardware-induced offsets and noise. Depending on the application, additional *signal transformations* (e.g., short-time Fourier transform, Doppler or body-velocity profiles [12]) may be applied to derive motion-sensitive representations. The resulting feature tensors form the input to a *machine learning model*, typically a convolutional or a recurrent network, which maps temporal and/or spatial channel variations to semantic outputs such as human activity, gesture, or identity labels. The final *classification result* is produced at the application layer and can support downstream tasks such as authentication, occupancy detection, or behavior monitoring [16].

5) System / Deployment: privacy leakage, cross-device transfer, confidence manipulation
4) ML model: model extraction, poisoning, backdoors, evasion
3) Data / Pre-processing: phase sanitization exploits, transform-domain perturbations, segmentation or window manipulation
2) Network layer: packet modification, dropping, timing manipulation
1) Physical layer: signal injection, jamming, replay, hardware tampering

Figure 2: Taxonomy of threat models in CSI-based sensing

2.3 Threat Landscape in Wi-Fi Sensing

The pipeline of Wi-Fi sensing introduces multiple points of vulnerability that adversaries can exploit. These threats span five layers, reflecting both the wireless protocol stack and the ML hierarchy.

Referring to Figure 2, at the *physical layer*, attackers can perform signal injection, jamming, or replay to distort the measured channel. Moving upward, the *network layer* exposes the system to packet-level manipulation, such as selective dropping or timing alteration, which can corrupt CSI acquisition. The *data or pre-processing layer* can be targeted through phase-sanitization exploits, transform-domain perturbations, or segmentation tricks that manipulate the data fed to downstream models. The *ML model layer* is vulnerable to training-time and inference-time attacks including classical adversarial techniques such as extraction, membership inference, backdoors, poisoning, and evasion attacks. Finally, at the *system or deployment layer*, adversaries may exploit cross-device transfer, privacy leakage, or confidence manipulation to compromise system integrity or trustworthiness. Understanding how these attack surfaces interact is critical for designing end-to-end robust Wi-Fi sensing systems. We focus on the ML model layer.

2.4 Adversarial Machine Learning

Within adversarial machine learning (AML), the category of attacks where an adversary manipulates test-time inputs to induce misclassification is termed *evasion*. According to a recent NIST report on AML, evasion attacks are broadly classified by the threat model into *white-box* and *black-box* [34].

In the white-box setting, the attacker has full knowledge of the target model (architecture, hyperparameters, and training data). This represents a strong attacker and is the most commonly studied threat model, as it allows evaluation under worst-case assumptions. Conversely, the black-box setting assumes only minimal access, e.g., query interfaces, representing a more realistic but weaker adversarial position. We can taxonomize them further as follows [35]:

White-box evasion attacks:

- **Optimization-based attacks**, where adversaries solve a constrained optimization problem to maximize model loss while bounding perturbations, often expressed as

$$x^* = x + \delta \quad \text{s.t.} \quad \|\delta\|_p < \epsilon, \quad \arg \max f(x^*) \neq y, \quad (3)$$

where x is the original input, f the model, y the ground truth, and ϵ the perturbation budget for the ℓ_p norm.

- **Universal perturbations**, refer to a single perturbation vector (or patch) transferable across most inputs, typically via iterative optimization on a representative data subset.
- **Physically realizable attacks**, designed to survive domain distortions. In wireless sensing, a difficulty is that perturbations injected in the Radio Frequency (RF) domain may not map linearly into the model input space due to quantization, filtering, and multipath distortion.

Black-box evasion attacks:

- **Score-based attacks**, where the adversary leverages access to model logits or probabilities to approximate gradients.
- **Decision-based attacks**, which operate under access to only the final predicted labels and iteratively approximate decision boundaries.
- **Transfer-based attacks**, where adversaries train surrogate models or ensembles and transfer adversarial examples to the target system.

A range of defense strategies have been proposed to mitigate evasion attacks. Of these, the one which has stood the test of time and is scalable, is *adversarial training* [36]. According to this technique, adversarial examples incorporated during training can improve robustness. *Regularization-based methods*, such as enforcing consistency across perturbed and clean inputs, can further stabilize model predictions [37]. *Input transformations* (e.g., filtering or denoising) aim to remove adversarial noise prior to inference [38, 39], while *certified defenses* provide provable robustness guarantees under bounded perturbations [40, 41].

2.5 Security & Privacy Issues of Wi-Fi Sensing

While Wi-Fi-based human sensing has many benign applications (e.g., localization, gesture-based authentication, and elderly fall detection), its misuse raises significant security and privacy concerns. The upcoming IEEE 802.11bf standard will likely accelerate deployment, making these risks more pressing.

Malicious actors could deceive gesture-based authentication by replaying or spoofing activities, use passive sensing to infer occupancy or behaviors in sensitive environments, or disrupt safety-critical HAR systems (e.g., fall detection or occupancy-based emergency control). Adopting the perspective of a previous work [17], Wi-Fi sensing can be viewed from three angles: *sword*, *shield*, *victim*.

- **Sword (attacker)**: CSI can be exploited as a side-channel to infer identity, presence, or activities without consent, or perturbed to induce misclassifications in deployed models.
- **Shield (defender)**: Robust models and defenses (e.g., adversarial training, filtering strategies) are required to harden Wi-Fi sensing against these attacks.

- **Victim (user/system)**: End-users face potential privacy loss (e.g., covert occupancy detection), security breaches (e.g., gesture authentication spoofing), or safety hazards (e.g., adversarial interference with fall-detection alarms).

The importance of defending CSI-based sensing is underscored by its dual-use nature: the same fidelity that enables rich activity recognition also amplifies ethical/privacy risks of surveillance and adversarial exploitation. Therefore, understanding vulnerabilities (sword), developing countermeasures (shield), and mitigating harms (protecting the victim) are critical to its trustworthy adoption.

3 Related Work

3.1 Overview

While early work prioritized sensing fidelity, accuracy and scalability, recent efforts emphasize advanced modeling pipelines – environment generalization [42, 21, 43], few-/zero-shot learning [44, 45] and cross-application frameworks [46, 47] – and edge and/or federated deployments for heterogeneous IoT contexts [48, 49, 50]. Real-world systems are now expected to be adaptable to new users, environments, and configurations without exhaustive retraining.

In parallel, a growing body of work has been exploring how these systems behave when exposed to malicious interference or perturbations. However, security and privacy research in this area has been fragmented – spanning PHY layer manipulation, crafted RF signal injections, and adversarial ML attacks. To clarify this landscape, we begin by synthesizing prior works into *attack classes*, and use them to articulate the motivations for our work.

3.2 Attack Classes for Human-Centered Wireless Sensing

Several studies have proposed attack vectors and highlighted the vulnerabilities of Wi-Fi-based sensing systems to adversaries aiming to undermine privacy, integrity, or availability. Adapting prior taxonomies of human-centered wireless sensing (HWCS) [10] and [51], these threats can be broadly grouped into two categories: inference attacks and signal injection attacks.

3.2.1 Inference Attacks

Attackers can infer private information such as human presence, gestures, or even physiological signals without consent, exploiting the very properties that make Wi-Fi sensing convenient: open standards, ubiquity, device-free/pассиве operation, and minimal user cooperation. These attacks range in scope:

- *Small-scale*: keystroke detection [52] and vital sign monitoring, e.g., heart rate, respiration, sleep position, etc. [53];
- *Medium-scale*: gesture/activity recognition [54, 12, 55].

- *Large-scale*: people counting [56], occupancy detection [57], gait-based/person identification [58, 59]

3.2.2 Signal Injection Attacks

Attackers with transmission capabilities can escalate from passive inference to active disruption by injecting crafted RF signals into the environment. These signal injection or **spoofing** attacks are, by definition, *physically realizable*, since they operate directly through the wireless channel and therefore must obey its propagation, synchronization, and power constraints. By distorting the measured channel state, such attacks can degrade or deny the availability of legitimate sensing systems [60, 27]. Similar mechanisms may also be used defensively, for example, by injecting controlled noise to mask sensitive user motion or suppress unwanted inference [61].

A range of over-the-air (OTA) attack and defense mechanisms demonstrate how adversaries can steer receiver-side CSI while preserving normal communication links. Examples include Aegis, a privacy-preserving RF shielding system [62]; FooLoc, which models multiplicative propagation effects under channel constraints for localisation and fingerprinting [63]; WiAdv, which performs gesture spoofing using full-duplex radios [8]; PhyCloak, which obfuscates human motion signatures using a secondary SDR transmitter [60]; Wi-Spoof, which manipulates transmission power via pseudo pulse-width modulation to emulate fabricated activities [27]; and Li et al., who modify Wi-Fi preambles to corrupt channel estimation [64]. Beyond Wi-Fi CSI, RAFA provides a hardware OTA platform that accounts for channel transforms and synchronization [65], while channel-aware attacks under fading formalize power-limited adversaries [66]. Collectively, these works highlight the need for physics-guided constraints—such as coherence time/bandwidth, spatial correlation, and perturbation-to-signal ratio (PSR) limits—when defining realistic threat models.

3.3 Adversarial Perturbations in the Signal Domain

Adversarial Machine Learning (AML) extends these ideas to the data and model layers. Early gradient-based attacks remain the most widely used [7, 36, 67], and although designed for vision tasks, many have since been adapted to sequential data [68, 69], where perturbations must respect temporal smoothness and signal continuity.

Applying such threats to Wi-Fi sensing introduces additional challenges: CSI is complex-valued, high-dimensional, and non-stationary. Prior work shows that both white- and black-box attacks can reliably degrade model performance [28, 70], yet most methods ignore physical-layer constraints such as channel propagation, multipath structure, and transceiver behavior, limiting real-world feasibility. A smaller subset does account for these factors – e.g., WiCAM’s surrogate-based black-box attacks [26], and WiIntruder’s universal perturbations resilient to synchronization offsets [9]. Despite these recent advances, the field still lacks a unified robustness evaluation framework.

3.3.1 Assumptions and Threat Models

Most works assume an attacker can place an SDR or Wi-Fi transceiver in the environment. Depending on capability, the adversary may be *Rx-only* (passive) or *Tx/Rx* (active OTA injection), and may have *white-box* access to models/data or operate in *black-box/transfer* regimes. Our evaluation adopts this layered perspective to assess robustness across diverse attacker capabilities.

3.4 Lightweight Modeling for Wi-Fi Sensing

Under the emerging IEEE 802.11bf standard, CSI will be captured and preprocessed directly on access points and IoT devices. This shift raises a central systems question: “where will sensing inference actually run?” Edge devices typically operate under tight latency, memory, and energy constraints, and large-scale environments may require dozens of sensing nodes – greatly increasing the attack surface. These realities make lightweight, efficient and robust models essential for real-time operation, multi-node scalability, and privacy-preserving on-device processing.

Motivated by these requirements, several works have proposed *lightweight* or *edge-friendly* architectures for CSI-based sensing. Youm and Go [71] adopt neural architecture search and structured pruning to design compact HAR models; LiteHAR [72] replaces heavy backpropagation with random convolution kernels and ridge regression; LiteWiHAR [73] targets embedded devices with a small-footprint design; and hybrid attention–pruning approaches [74] and edge–cloud partitioning frameworks such as EfficientFi [75] further reduce computation and communication overhead.

Despite this progress, existing lightweight approaches primarily focus on architectural compression and inference-time efficiency. Much less attention has been given to the deeper modeling challenge inherent to Wi-Fi sensing: CSI provides extremely high-dimensional, complex-valued inputs, yet datasets remain relatively small and difficult to collect. Lightweight models that lack robustness may fail unpredictably under distribution shifts or malicious perturbations, underscoring the need to consider efficiency and robustness together rather than as separate design objectives.

3.5 Summary and Motivation

Existing robustness-oriented research in wireless sensing has explored the effects of signal injections and adversarial attacks. However, these studies often isolate specific models or datasets and neglect the physical realism of perturbations. This paper builds upon these foundations by establishing a unified framework for CSI-based sensing, incorporating physically constrained perturbations and multiple attack regimes to provide a reproducible, system-level evaluation of adversarial robustness in device-free human-centered wireless sensing. Furthermore, our work analyzes the robustness of compact models from a *representation-level perspective*, i.e., models that mitigate the high feature-to-sample ratio inherent to CSI datasets while maintaining strong downstream performance.

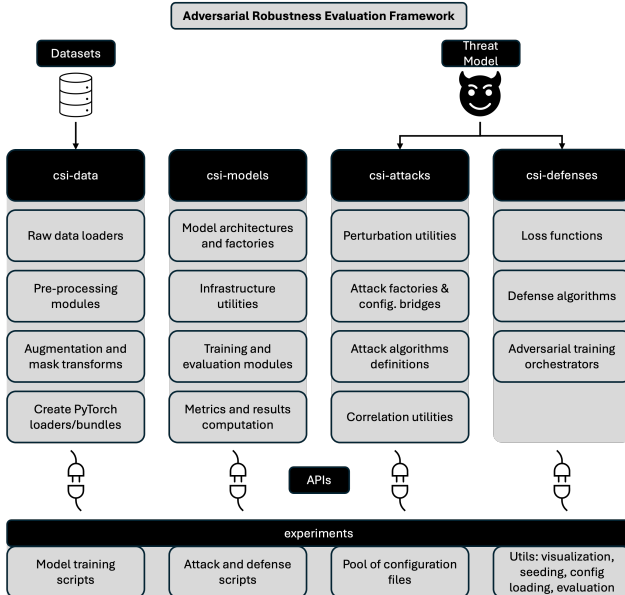


Figure 3: Modular framework under the `csi` namespace

4 Evaluation Framework

Our *Adversarial Robustness Evaluation Framework*, shown in Figure 3, is organized into modular layers that mirror the end-to-end Wi-Fi sensing and CSI ML adversarial robustness workflow. At its foundation, `csi-data` handles dataset ingestion, preprocessing, and augmentation through configurable loader bundles. `csi-models` defines the learning backbone, providing model factories, training loops, and evaluation metrics. `csi-attacks` encapsulates gradient- and score-based adversarial algorithms, along with correlation-preserving and physically grounded perturbation utilities. `csi-defenses` implements countermeasures, providing shared loss modules and adversarial trainers. These components form the foundation for the datasets, tools and algorithms described next, providing the infrastructure for our experiments.

The APIs are unified under an `experiments` layer that manages configuration files, training and evaluation scripts, and cluster orchestration for large-scale studies. Together, the framework enables reproducible experimentation on CSI datasets, supporting clean and adversarial evaluations, model comparison, and systematic analysis of robustness under varying threat models. The entire framework is implemented in Python, and relies on libraries such as PyTorch, NumPy, and YAML. An open-source release will be made available upon acceptance.

5 Methodology

For reproducibility, this paper’s benchmark improves upon another recent benchmark, SenseFi [76], which focused on building a public suite of deep-learning models for Wi-Fi human sensing. We were largely able to match the results reported in this work through our re-implementation of the models. To this, we added a suite of adversarial modules for attacks, defenses, and experimentation.

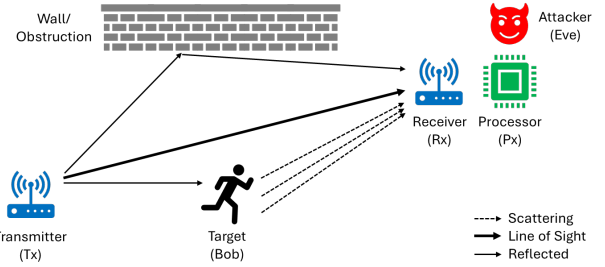


Figure 4: Threat model. P_x is compromised by Eve

5.1 Threat Model

We first define the threat model we use to assess the robustness of CSI-based ML models. We assume an adversary capable of compromising the platform at the point where processed CSI features are passed to the model, i.e., after raw CSI extraction but before inference. This aligns with integrity-focused attacks, where the attacker’s objective is to induce misclassification by manipulating the model’s inputs. Although prior work has explored threats at the physical or network layers – using RF signal injection or packet manipulation – we focus on this model-level access because it represents the strongest and most general capability: full control over the inputs that drive the decision-making model. This allows us to characterize the upper bound on the damage an adversary can inflict.

As seen in Figure 4, the system is comprised of four distinct parties: a transmitter (T_x), a receiver (R_x), a sensing target/human (Bob), and an adversary (Eve). Eve is assumed to be co-located with the model platform (P_x). However, since we are evaluating algorithmic robustness, the relative positions of these parties are not relevant – T_x , R_x and Bob may be in different rooms or in the same one. We assume that Eve wishes to disrupt/deny sensing by causing targeted/untargeted misclassification of the legitimate ML model, whilst minimizing the likelihood of detection by crafting perturbations that satisfy the physical constraints of real Wi-Fi signals and therefore resemble normal transmissions.

5.2 Datasets

The datasets that were used as part of the robustness evaluations are: University of Toronto Human Activity Recognition (**UT-HAR**) [77], Nanyang Technological University Human Activity Recognition and Human Identification (**NTU-HAR** and **NTU-HID**) [75, 78]. The three datasets are composed of CSI amplitudes, and they were all captured indoors. Despite this, their reason for selection for this benchmarking is that they are all well-recognized, recent datasets that accurately represent the capabilities of modern CSI processing hardware, and have been used extensively to train CSI ML models. Table 1 summarizes their properties.

Each dataset was split into training, validation, and test sets with a fixed seed and a 70/10/20 ratio (train-val-test). CSI amplitudes were standardized via per-subcarrier z -score normalization; temporal smoothing was applied only to the NTU datasets. Training batch sizes ranged between 32 and 64, while validation and test loaders used 64–128.

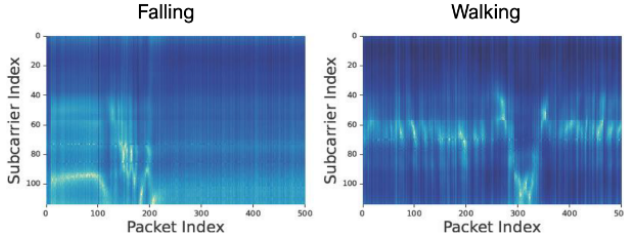


Figure 5: CSIs of human activities from NTU-HAR [76]

Table 1: CSI-based datasets for Wi-Fi sensing. Data is in the format of (Antenna, Subcarrier, Packet).

Datasets	UT-HAR	NTU-HAR	NTU-HID
Platform	Intel 5300 NIC	Atheros CSI Tool	Atheros CSI Tool
Categories	7	6	14
Labels	Lie down, Fall, Walk, Pick up, Run, Sit down, Stand up	Box, Circle, Clean, Fall, Run, Walk	Gaits of 14 Subjects
Data Size	(3,30,250)	(3,114,500)	(3,114,500)
Train Size	3977	936	546
Test Size	996	264	294
Train Epochs	100	100	100

5.3 Models

SenseFi baselines (Large) From the 11 SenseFi models, we deliberately choose three unique architectures because they capture different structural assumptions about CSI data – spatial, temporal, and hierarchical – providing complementary perspectives on model robustness, while keeping the suite compact and reproducible: **LeNet/CNN5** (convolutional baseline), **BiLSTM** (sequence model for temporal dependencies), and **ResNet-18** (deeper residual network adapted to CSI inputs). To ensure plug-and-play use across all datasets, we implement *custom model factories* that automatically configure input shapes, normalization layers and heads per dataset. They were each trained for up to 100 epochs using Adam (learning rate 10^{-3} , weight decay 5×10^{-4}) with early stopping (patience 25, min_epochs 40) based on validation loss.

Lightweight latent classifiers (Tiny) CSI tensors are high-dimensional (Table 1); to probe robustness–capacity trade-offs, we devise a second pathway that trains *tiny* classifiers in two stages: (i) a **TCN bottleneck autoencoder** for temporal dimensionality reduction, then (ii) swap the decoder with a classifier head operating on the compressed latent. We evaluate three heads: a **TCN** (lightweight temporal baseline using causal/dilated convolutions), a **GRU** (compact gated recurrent unit with fewer parameters than LSTM), and a **State-Space Model (SSM)** implemented in the modern structured state-space style (S4-inspired) for stable long-range dependencies with linear-time inference. The encoder is shared across heads; heads are re-initialized per dataset via the same model factories, yielding consistent data handling and enabling fair comparisons between the

lightweight models and the larger SenseFi baselines.

The encoder was trained with a mixed reconstruction loss combining mean-squared error, masked region weighting (mask_focus 1.0 \rightarrow 0.0 over 40% of training), and a contractive regularization term $\lambda \|\partial z / \partial x\|_F^2$ with $\lambda = 2 \times 10^{-4}$ applied every 4 steps to 50% of samples. Optimization used Adam (learning rate 10^{-3} , weight decay 5×10^{-4} , gradient clip 1.0) for 100 epochs with early stopping (patience 25). Fine-tuning followed a two-phase schedule: Phase A froze the encoder (10 epochs, head LR 2×10^{-3}); Phase B unfroze all weights (30 epochs, head LR 2×10^{-3} , encoder LR 2×10^{-4}) using a Reduce-on-Plateau scheduler (factor 0.5, patience 5).

5.4 Adversarial Attacks

We evaluate a compact suite of adversaries that cover strong white-box, practical black-box, and input-agnostic threat classes. Concretely, we test: (i) first-order **white-box attacks (PGD)** in both *untargeted* and *targeted* modes to probe gradient sensitivity across architectures and model capacities; (ii) **DeepFool** [79], an *untargeted* ℓ_2 - minimal perturbation method used to expose local decision-boundary geometry; (iii) **universal adversarial perturbations (UAPs)** [80], which are inherently *untargeted* and evaluate input-agnostic interference patterns across samples; and (iv) **transfer attacks** – conducted in both *targeted* and *untargeted* forms – to quantify black-box risk through intra-family and inter-family surrogate transfer, simulating model-stealing or surrogate-training scenarios.

Let $\mathcal{D} = \{(x_i, y_i)\}_{i=1}^N$ be the labeled dataset, where $x_i \in \mathcal{X}$ denotes an input (CSI/representation) and $y_i \in \mathcal{Y}$ its ground truth. A classifier $f_\theta : \mathcal{X} \rightarrow \mathbb{R}^K$ produces logits $f_\theta(x)$, with prediction $\hat{y} = \arg \max_k f_\theta(x)_k$. An adversarial perturbation δ seeks to alter the output while remaining within a bounded set $\|\delta\|_p \leq \varepsilon$. In *untargeted* attacks, the goal is $\hat{y}(x + \delta) \neq y$, whereas in *targeted* attacks, $\hat{y}(x + \delta) = y_{\text{tgt}}$. Below we give short descriptions of each attack setting. We refer the reader to the original papers and our software implementation for all the full algorithms.

DeepFool (untargeted, ℓ_2 -minimal) Linearize f_θ at $x^{(t)}$; for each $k \neq \hat{y}$:

$$r_k^{(t)} = \frac{f_\theta(x^{(t)})_{\hat{y}} - f_\theta(x^{(t)})_k}{\|\nabla_x f_\theta(x^{(t)})_{\hat{y}} - \nabla_x f_\theta(x^{(t)})_k\|_2^2} \times (\nabla_x f_\theta(x^{(t)})_{\hat{y}} - \nabla_x f_\theta(x^{(t)})_k) \quad (4)$$

Pick $r_{k^*}^{(t)}$ with smallest norm, set $x^{(t+1)} = x^{(t)} + r_{k^*}^{(t)}$ until class changes; $\delta = x^{(T)} - x$.

Projected Gradient Descent (PGD) Maximize the loss within the norm ball:

$$\delta^* = \arg \max_{\|\delta\|_p \leq \varepsilon} \mathcal{L}(f_\theta(x + \delta), y) \quad (5)$$

Return $\delta = g^{(T)}$, using iterative ascent/descent updates:

$$g_{\text{untgt}}^{(t+1)} = \Pi_{\|\cdot\|_p \leq \varepsilon} \left(g^{(t)} + \alpha \text{sign}(\nabla_x \mathcal{L}(f_\theta(x + g^{(t)}), y)) \right),$$

$$g_{\text{tgt}}^{(t+1)} = \Pi_{\|\cdot\|_p \leq \varepsilon} \left(g^{(t)} - \alpha \text{sign}(\nabla_x \mathcal{L}(f_\theta(x + g^{(t)}), y_{\text{tgt}})) \right).$$

Universal Adversarial Perturbations (UAP) Find universal vector v with $\|v\|_p \leq \xi$ such that

$$\Pr_{x \sim \mathcal{D}}(\hat{y}(x + v) \neq \hat{y}(x)) \geq 1 - \delta \quad (6)$$

Iteratively, if $x_i + v$ is still correct, add the minimal Δv_i (e.g., DeepFool) and project:

$$v \leftarrow \Pi_{\|\cdot\|_p \leq \xi}(v + \Delta v_i) \quad (7)$$

Transfer Attacks Generate adversarials on a surrogate and then evaluate on a target. We consider *intra-family* (same architecture type) and *inter-family* (different inductive biases) transfer in both untargeted and targeted modes.

Algorithm 1 Physically Constrained Projection $\Pi_{\text{phys}}(\delta)$

Require: perturbation $\delta \in \mathbb{R}^{K \times T}$ (or $K \times T \times N_a$), clean batch X , norm bound ε
Ensure: projected perturbation $\tilde{\delta}$

1: **Frequency correlation (PDP-based):**

2: Construct Toeplitz matrix C with entries

$$C_{ij} = \begin{cases} \exp(-(2\pi\tau_{\text{rms}}|f_i - f_j|)^2), & \text{Gaussian PDP,} \\ (1 + (2\pi\tau_{\text{rms}}|f_i - f_j|)^2)^{-1/2}, & \text{Exponential PDP.} \end{cases}$$

3: Normalize $\text{diag}(C) = 1$, then set $\delta \leftarrow C\delta$.

4: **Temporal smoothing (Doppler constraint):**

5: Apply convolution along time dimension t :

$$\delta(k, t) \leftarrow (\delta(k, \cdot) * g_{\sigma_t})(t), \quad g_{\sigma_t}(t) \propto e^{-t^2/(2\sigma_t^2)}.$$

6: **Spatial/MIMO correlation:**

7: Estimate covariance $\mathbf{R}_{\text{rx}} = \mathbb{E}[\mathbf{h}\mathbf{h}^H]$ from clean CSI or a regularized prior.

8: Factorize $\mathbf{R}_{\text{rx}} = \mathbf{L}\mathbf{L}^H$ (Cholesky) and apply per (k, t) :

$$\delta_{k,t,:} \leftarrow \delta_{k,t,:} \mathbf{L}^T.$$

9: **Distributional alignment (MMD penalty):**

10: Compute mini-batch MMD between clean X and perturbed $Y = X + \delta$:

$$\widehat{\text{MMD}}^2(X, Y) = \frac{1}{m(m-1)} \sum_{i \neq j} [k(x_i, x_j) + k(y_i, y_j)] - \frac{2}{m^2} \sum_{i,j} k(x_i, y_j),$$

where $k(u, v) = \exp(-\gamma\|u - v\|_2^2)$, $\gamma = (2\sigma^2)^{-1}$.

11: **ℓ_2 normalization and projection:**

12: Final energy projection onto norm ball:

$$\tilde{\delta} = \varepsilon \frac{\delta}{\|\delta\|_2}.$$

13: **return** $\tilde{\delta}$.

Perturbation Constraints We adopt the Euclidean (ℓ_2) norm as the distance metric between clean and perturbed signals, owing to its natural interpretation as signal energy.

Accordingly, we define the *Perturbation-to-Signal Ratio* (PSR) as:

$$\text{PSR} = -\text{SNR} = 10 \log_{10} \left(\frac{\|\delta\|_2^2}{\|x\|_2^2} \right) \quad (8)$$

where x and δ denote the clean and adversarial signals, respectively. Higher PSR values indicate stronger perturbations relative to the signal energy and thus correspond to lower effective *Signal-to-Noise Ratios* (SNR). In practice, an attack budget specified as a target SNR (e.g., 20 dB) is converted to its equivalent ℓ_2 ratio – we derive an absolute norm bound per sample as $\varepsilon = \varepsilon_{\text{rel}}\|x\|_2$, $\varepsilon_{\text{rel}} = 10^{-\text{SNR}_{\text{dB}}/20}$.

A strong, stealthy attacker must ensure that any perturbations they introduce remain consistent with the physical constraints of the RF channel; large or statistically implausible deviations in CSI would be easily detectable or physically unrealizable. To model these constraints, we apply a physics-guided projection operator Π_{phys} after each adversarial update, as specified in Algorithm 1.

Its first three steps impose frequency, temporal, and spatial coupling consistent with the coherence bandwidth, coherence time, and MIMO correlation structure of indoor Wi-Fi channels. These correlations capture how multipath spreads energy across neighboring subcarriers, how slowly time-varying channels evolve across OFDM symbols, and how antenna elements observe partially overlapping propagation paths. Under the WSSUS (Wide-Sense Stationary Uncorrelated Scattering) assumption, the frequency correlation function is the Fourier transform of the PDP, yielding the Gaussian/Lorentzian forms used in our Toeplitz subcarrier correlation model [81]; coherence time scales inversely with Doppler, motivating temporal low-pass smoothing; correlated MIMO motivates imposing a receive covariance via Cholesky factorization [82].

Step 4 uses an RBF-kernel MMD loss to keep the perturbed samples $(X + \delta)$ close to the empirical clean data manifold [83], a technique also employed in CSI domain-alignment pipelines [84, 85]. Finally, Step 5 bounds the perturbation energy using PSR, consistent with OTA practice [64, 63], by projecting onto the ℓ_2 ball. The resulting composite operator serves as a proximal constraint applied after each adversarial update to ensure physical plausibility and prevent divergence from realistic wireless behavior:

$$\Pi_{\text{phys}}(\delta) = \Pi_{\ell_2} \left(\Pi_{\text{spatial}} \circ \Pi_{\text{temporal}} \circ \Pi_{\text{frequency}}(\delta) \right) \quad (9)$$

Implementation Details PGD, DeepFool, UAP, and transfer attacks were generated with shared budgets corresponding to 10–40 dB PSR ($\varepsilon = 10^{-\text{PSR}/20}$). PGD used 100 steps (step size controlled by `alpha_fraction`= 1.0, i.e., $\alpha = \varepsilon/10$) and 5 random restarts. DeepFool ran for 100 iterations (overshoot 0.02). UAPs used 5 outer passes with a target fooling rate of 0.9 and 50 mini-batches for mean-norm estimation. Correlation preservation was enabled for UAPs, whereas only the dedicated PGD-Corr variant included an additional MMD term with weight $w_{\text{MMD}} = 0.25$.

5.5 Adversarial Defenses

We adopt **adversarial training (PGD-AT)** and its **TRADES** variant, both optimizing robustness under bounded perturba-

tions $\|\delta\|_p \leq \varepsilon$. Let f_θ be trained on \mathcal{D} with loss \mathcal{L} .

Adversarial Training (PGD-AT)

$$\min_{\theta} \mathbb{E}_{(x,y) \sim \mathcal{D}} \left[\max_{\|\delta\|_p \leq \varepsilon} \mathcal{L}(f_\theta(x + \delta), y) \right] \quad (10)$$

PGD approximates the inner maximization; the outer step updates θ on $x + \delta$.

TRADES (natural–robust trade-off)

$$\begin{aligned} \min_{\theta} \mathbb{E}_{(x,y) \sim \mathcal{D}} & \left[\underbrace{\mathcal{L}(f_\theta(x), y)}_{\text{clean accuracy}} \right. \\ & \left. + \beta \underbrace{\max_{\|\delta\|_p \leq \varepsilon} \text{KL}(f_\theta(x) \parallel f_\theta(x + \delta))}_{\text{robustness term}} \right] \end{aligned} \quad (11)$$

where $\beta > 0$ balances clean and robust performance by enforcing prediction consistency under perturbations using the Kullback–Leibler (KL) term.

Implementation Details PGD-AT minimized cross-entropy under a 20 dB PSR perturbation with 20 PGD inner steps (step $\alpha = \varepsilon/10$, 5 restarts). TRADES used the same inner attack with $\beta = 2.0$ and a KL-divergence loss. Both were trained with Adam (10^{-3} , weight decay 5×10^{-4}) and early stopping on robust validation accuracy. All experiments were executed on a desktop-class GPU.

5.6 Evaluation Metrics

To evaluate the impact of adversarial attacks and the effectiveness of defenses, we adopt the following metrics:

Attack Success Rate (ASR) The fraction of inputs that are misclassified after adversarial perturbation:

$$\text{ASR} = \frac{1}{N} \sum_{i=1}^N [f_\theta(x_i + \delta_i) \neq y_i] \quad (12)$$

Accuracy (Acc) and Robust Accuracy (RAcc) The standard top-1 classification accuracy on clean test data (Acc) and classification under adversarial attack (RAcc):

$$\text{Acc} = \text{RAcc} = \frac{1}{N} \sum_{i=1}^N [\hat{y}_i = y_i] \quad (13)$$

where $\hat{y}_i = \arg \max_k f_\theta(\text{input})_k$ is the predicted label and y_i the ground truth. By construction, RAcc = 1 – ASR when evaluated on correctly classified clean inputs.

For completeness, we also report **F1 score (F1)** which is particularly relevant for imbalanced datasets. Furthermore, when comparing models of different sizes, we report their **model capacity**, defined as the total number of trainable parameters.

Table 2: Macro F1 score (%) with parameter counts

Model (Params)	UT-HAR	NTU-HAR	NTU-HID
TCN AE (28.8K)	93.83	96.20	97.27
SSM AE (36.3K)	92.87	95.82	90.86
GRU AE (82.0K)	94.79	95.49	96.22
BiLSTM (227.1K)	95.19	95.04	99.31
LeNet (619.8K)	96.82	96.98	100.0
ResNet18 (11.17M)	96.82	95.14	100.0

6 Results

Owing to the large number of configurations/parameters to sweep, each setup – repeated across five random seeds for rigor – was executed on high-performance cluster compute nodes, each with up to 16GB of RAM and desktop GPUs (e.g., NVIDIA RTX 4070).

6.1 Clean Model Baseline

We first evaluated the clean performance of all models across the three datasets: UT-HAR, NTU-HAR and NTU-HID. Table 2 summarizes the macro F1-score and model size. Despite being $10\text{--}100\times$ smaller, the *tiny* models (TCN, GRU, SSM) achieve comparable – and occasionally superior – performance to the *large* baselines (ResNet18, BiLSTM, LeNet).

Key Takeaways

Model capacity alone does not dictate representational quality for raw CSI-based sensing.

6.2 White-Box Robustness Benchmarking

We next evaluated model robustness under full knowledge (white-box) adversaries, i.e., the strongest attacker, using several ℓ_2 -bounded attacks, such as PGD $_{\ell_2}$ (or **PGD**), **PGD-Corr** (with $\Pi_{\text{phys}}(\delta)$), and **DeepFool**, across targeted and untargeted settings. Targeted attacks refer to *pairwise* attacks with 1–1 mapping between label sources and targets. Each attack is executed at Signal-to-Perturbation Noise ratio (SNR) budgets of 10 dB, 20 dB, and 40 dB.

We make the following key observations from Table 3 and Figure 6: 1) larger perturbation budgets lead to higher ASR; 2) ASRs were broadly comparable across datasets, with NTU-HID (14 classes) being the least vulnerable; 3) With a limited budget, the ease with which we can *conceal* (given source to any other target) or *promote* (given target from any other source) classes is a property of the data distribution; 4) Applying physical constraints like smoothing and distribution matching through PGD-Corr attacks almost entirely neutralized the attacks and caused a drastic drop in the attack performance of the algorithms to at most 5%, even for the strongest perturbations (10 dB); 5) Untargeted attacks had a marginally higher ASR than targeted attacks which require a precise move from a particular source class to a target class; 6) Our tiny models were found to exhibit consistently lower robustness than the larger baseline models across all budgets.

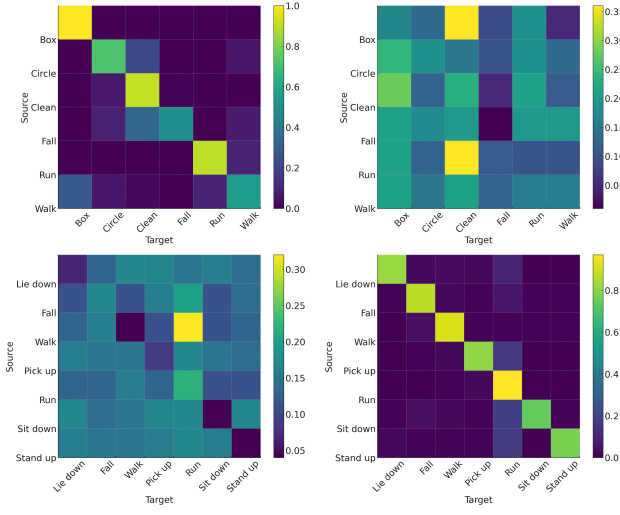


Figure 6: Very different *concealment* and *promotion* performance with ResNet18: NTU-HAR (above) & UT-HAR (below)

Table 3: Mean (μ) \pm SD of Adversarial Success Rate (ASR, %) for white-box attacks across perturbation budgets and methods.

Setting	UT-HAR	NTU-HAR	NTU-HID
Effect of perturbation budget			
10 dB	62.3 \pm 46.0	61.1 \pm 45.6	52.7 \pm 45.6
20 dB	55.8 \pm 43.7	44.6 \pm 40.5	34.4 \pm 36.9
40 dB	5.7 \pm 7.7	4.5 \pm 6.2	2.5 \pm 3.9
Effect of attack method			
DeepFool	65.1 \pm 38.8	58.8 \pm 37.0	52.3 \pm 36.0
PGD	57.4 \pm 41.7	47.6 \pm 41.1	33.8 \pm 36.4
PGD-Corr	0.2 \pm 0.4	0.2 \pm 0.3	1.0 \pm 0.3
Effect of attack target			
Untargeted (PGD & DF)	67.1 \pm 40.4	61.3 \pm 40.3	57.4 \pm 40.7
Targeted (PGD)	57.4 \pm 41.7	47.6 \pm 41.1	33.8 \pm 36.4
Effect of model size			
Tiny	42.9 \pm 43.2	41.7 \pm 43.9	30.4 \pm 40.1
Large	35.9 \pm 44.4	26.9 \pm 38.2	25.6 \pm 37.9

Key Takeaways

The tiny models were considerably less robust than the larger baselines. Applying physical constraints almost entirely neutralized the adversarial examples’ potency.

6.3 Black-Box Transfer Attacks

We evaluated the *transferability* of adversarial perturbations under both *intra-family* (tiny and large) and *inter-family* (tiny \leftrightarrow large) black-box settings. We consider PGD $_{\ell_2}$ and DeepFool attacks with 10, 20, and 40 dB budgets, and evaluate them in both untargeted and targeted configurations. Transferability provides insight into the degree of shared decision boundaries across model architectures, with a higher ASR implying that attackers can more easily generate effective adversarial examples using surrogate models trained on the same datasets as the target model.

Table 4: Mean (μ) \pm SD of ASR (%) for **intra-family** black-box transfers across different SNR budgets

Mode	10 dB	20 dB	40 dB
Tiny			
Untargeted	83.20 \pm 5.58	57.10 \pm 12.07	4.10 \pm 1.81
Targeted	67.92 \pm 6.73	38.65 \pm 9.21	2.08 \pm 1.26
Large			
Untargeted	16.23 \pm 11.59	2.21 \pm 1.38	0.14 \pm 0.16
Targeted	5.72 \pm 3.73	0.96 \pm 0.64	0.07 \pm 0.13

Table 5: Mean (μ) \pm SD of ASR (%) for **inter-family** transfers across different SNR budgets

Mode	10 dB	20 dB	40 dB
Tiny \rightarrow Large			
Untargeted	9.59 \pm 13.45	0.60 \pm 0.70	0.01 \pm 0.04
Targeted	3.72 \pm 3.68	0.34 \pm 0.23	0.01 \pm 0.03
Large \rightarrow Tiny			
Untargeted	15.98 \pm 9.85	2.50 \pm 1.26	0.16 \pm 0.17
Targeted	10.57 \pm 5.46	1.91 \pm 1.12	0.11 \pm 0.14

Intra-Family Transferability From the results in Table 4, we can infer that there is a sharp contrast in the transferability ASR between the tiny AE-head models (high) and the larger baselines (low). Even at 10 dB SNR, there is almost no intra-family transfer for the larger models. These findings highlight strong feature-space alignment within the tiny model family but highly distinct decision manifolds across larger CNN/LSTM architectures.

Inter-Family Transferability. Next, from Table 5, we observe that there is comparable transferability of adversarial examples between the model families – with the *Large \rightarrow Tiny* having marginally greater success. Yet again, at 40 dB SNR, the transferability is very low ($\approx 0\%$), and this increases to ($\approx 13\%$) at 10 dB SNR. Comparing the datasets, we found that the adversarial examples were significantly more transferable with the UT-HAR dataset (≈ 3 times).

Key Takeaways

The transferability strongly depends on model architecture (and scale, here). The high intra-family ASR among AE-heads is validated by the shared latent structure imparted by training.

6.4 Universal Adversarial Perturbations

We investigated the efficacy of Universal Adversarial Perturbations (UAPs), another variant of black-box attacks, generated with a maximum perturbation budget of 10 dB SNR. These universal perturbations are designed to generalize across users, gestures, and environments. Table 6 summarizes the results.

Without any realism constraints, naïve UAPs achieve a high mean ASR of $48.3 \pm 21.1\%$, indicating that an attacker could, in principle, severely compromise a model’s predictions with a single, carefully crafted perturbation sig-

Table 6: Mean (μ) \pm SD of ASR (%) with Universal Adversarial Perturbations (UAPs) at SNR = 10 dB

Corr/Aggr	UT-HAR	NTU-HAR	NTU-HID	ASR
F F	61.5 \pm 17.3	45.0 \pm 23.1	38.6 \pm 17.3	48.3 \pm 21.1
F T	41.5 \pm 20.1	33.2 \pm 28.5	20.4 \pm 8.8	31.7 \pm 21.4
T F	20.2 \pm 6.2	32.5 \pm 19.2	14.5 \pm 14.4	22.4 \pm 15.7
T T	0.5 \pm 1.2	0.8 \pm 1.6	1.1 \pm 2.5	0.8 \pm 1.8
Tiny	40.0 \pm 29.1	42.7 \pm 23.9	27.4 \pm 20.2	36.7 \pm 25.1
Large	22.3 \pm 18.0	11.0 \pm 12.0	9.5 \pm 8.2	14.3 \pm 14.2

Table 7: Mean (μ) \pm SD of ASR, Clean and Robust F1 Scores (%) of the tiny & large model sets with PGD-AT & TRADES

Family	Metric	UT-HAR	NTU-HAR	NTU-HID
Tiny – PGD-AT	ASR	26.1 \pm 1.6	17.7 \pm 2.6	22.2 \pm 4.7
	Clean F1	75.4 \pm 3.5	95.0 \pm 1.2	91.8 \pm 3.2
	Adv F1	59.5 \pm 3.0	76.3 \pm 2.4	72.0 \pm 6.3
Tiny – TRADES	ASR	32.8 \pm 5.1	16.4 \pm 1.2	27.1 \pm 1.9
	Clean F1	85.9 \pm 2.9	95.1 \pm 0.4	91.4 \pm 2.8
	Adv F1	62.2 \pm 2.2	78.1 \pm 1.5	67.0 \pm 4.4
Large – PGD-AT	ASR	12.2 \pm 2.8	12.3 \pm 1.5	7.6 \pm 0.9
	Clean F1	97.8 \pm 1.2	97.6 \pm 2.0	98.4 \pm 0.9
	Adv F1	89.0 \pm 3.2	84.2 \pm 3.2	91.2 \pm 2.0
Large – TRADES	ASR	14.3 \pm 2.7	10.1 \pm 0.8	9.3 \pm 2.9
	Clean F1	96.4 \pm 0.6	96.3 \pm 1.4	97.9 \pm 1.4
	Adv F1	86.4 \pm 2.7	85.5 \pm 1.8	89.0 \pm 3.9

nal. However, enforcing realism – by aggregating per-batch updates to average out sample-specific artifacts and by preserving channel correlations – had a substantial impact on ASR, reducing it to just $0.8 \pm 1.8\%$. The tiny models exhibited considerably greater vulnerability than the larger baselines. Overall, none of our datasets were resistant to UAPs.

Key Takeaways

Naïve UAPs were found to be fairly effective across model architectures and datasets. Adding realism to UAPs through per-batch aggregates and correlation preservation reduced ASR dramatically. The tiny AE-based models were more vulnerable to UAPs as well.

6.5 Adversarial Training and Robustness Augmentation

Having investigated several ways of compromising model integrity, we next evaluated two robustness-augmentation strategies under a 20 dB PGD-L₂ threat: standard adversarial training and TRADES. Table 7 summarizes the resulting clean and robust performance for both the model sets, allowing us to assess the trade-offs each defense technique introduces.

PGD-AT It was found to considerably improve robustness across all datasets with modest decreases in clean performance. The larger SenseFi models benefit the most, achieving low attack success and strong robust F1 while maintaining high clean accuracy.

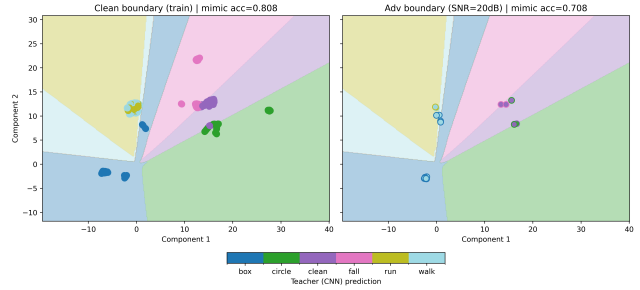


Figure 7: LeNet UMAP decision boundaries from a DistillMLP surrogate on NTU-HAR. Marker fill = true class, edge color = LeNet prediction. Untargeted PGD $_{\ell_2}$ attack (SNR = 20 dB)

TRADES It further stabilizes the clean–robust trade-off, offering slightly improved robustness at comparable or better clean accuracy. Tiny models show the largest proportional gains, while the large models retain strong clean and robust performance.

Key Takeaways

PGD-AT and TRADES both substantially improve robustness under PGD-L₂ attacks. PGD-AT delivers the largest raw reduction in attack success, whereas TRADES provides a more balanced clean–robust trade-off, making it particularly suitable for continuous CSI-based sensing deployments where maintaining high clean accuracy is essential.

6.6 Analysis of Adversarial Samples

We examined the decision boundaries of the trained models and how adversarial examples traverse them. Figure 7 visualizes the LeNet model and a DistillMLP surrogate on the NTU-HAR dataset after projecting feature representations into a two-dimensional UMAP space fitted on *clean data*. The background colors denote the surrogate’s decision regions, learned via knowledge distillation by minimizing the Kullback–Leibler divergence between its softmax outputs and the teacher’s stored probabilities. Scatter markers overlay adversarial examples generated with an untargeted PGD $_{\ell_2}$ attack (100 steps, 5 restarts, SNR = 20 dB). Comparing the two panels, we observe that perturbations push samples across decision boundaries into neighboring regions. The surrogate’s mimic accuracy drops from 80.8% to 70.8%, showing that a model distilled solely from clean embeddings cannot reproduce the teacher’s complex decision boundaries in regions exposed by adversarial attacks.

Figure 8 shows the effect of applying physical constraints on the perturbation patterns under the same untargeted PGD $_{\ell_2}$ attack. Each pixel represents the mean absolute perturbation $|\delta|$ across time (horizontal) and subcarrier index (vertical). Brighter regions reveal where the optimizer concentrates energy, e.g., within specific subcarrier groups that encode distinct motion dynamics. This structured pattern contrasts sharply with the noise-like appearance when correlation is preserved.

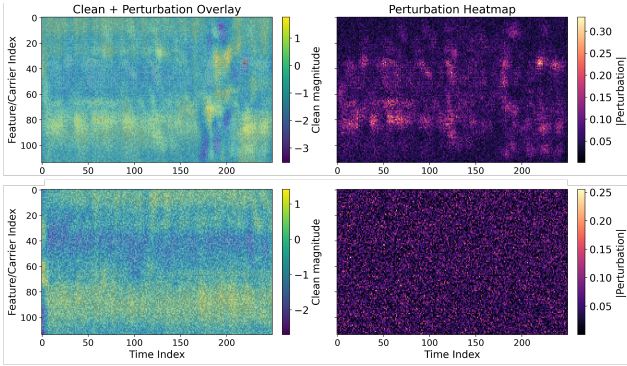


Figure 8: Perturbing from *walk* to *box* without (above) and with (below) physical constraints: PGD $_{\ell_2}$ attack (SNR = 20 dB)

Key Takeaways

Timeseries adversarial examples also systematically nudge samples across the model’s decision boundaries. Enforcing physical constraints and preserving correlation make the perturbations resemble random noise, weakening their ability to exploit structured vulnerabilities.

7 Discussion

7.1 Design Principles for Robust CSI Sensing

Our findings lead to several actionable design principles:

- 1. Model capacity is not a proxy for representational quality:** Though larger models were found to consistently be more robust, it is critical to understand how well the model decision boundaries are aligned with the geometric structure of CSI data.
- 2. Use of lightweight models requires dedicated robustness strategies:** The tiny/AE-based models showed significantly lower robustness. Lightweight deployments (e.g., 802.11bf) must therefore integrate robustness techniques rather than relying purely on efficiency/clean performance.
- 3. Physical constraints provide a natural defense:** Imposing spectral, temporal, and spatial plausibility nearly neutralized adversarial perturbations. Incorporating such constraints – whether during training or attack modeling (e.g., anomaly detection) – should be standard practice.
- 4. Universal perturbations must be prioritized:** Naïve UAPs were surprisingly effective across datasets and architectures. However, enforcing physical realism sharply reduced ASR, underscoring the need to evaluate both unconstrained and constrained UAPs.
- 5. Adversarial training remains a highly effective model defense:** PGD-AT achieved the largest reduction in ASR, whereas TRADES delivered a more favorable clean-robust trade-off – attractive for long-running sensing deployments.

7.2 Implications of Feature Engineering

The observed fragility of end-to-end CSI models underscores a fundamental tension between *robustness* and *generalization*. Existing feature-engineered pipelines – such as Widar3.0 [12] and SHARP [21] – aim to derive domain-invariant representations that enhance cross-environment or cross-user generalization. However, our findings suggest that such engineering – analogous with our AE representations – may inadvertently remove high-frequency or low-level statistical cues that are crucial for robust decision boundaries. This could make models less sensitive to semantically meaningful variations and leave them vulnerable to *feature-space poisoning* or distributional manipulation at training or test time.

Consequently, while feature engineering promotes convenience and portability, its effect on robustness – particularly under physically constrained or adversarial perturbations – remains underexplored. Future work should systematically assess whether feature engineering amplifies or mitigates vulnerability, and develop hybrid methods that combine *domain generalization* with *robust feature alignment*, potentially via certifiable or randomized invariance learning frameworks.

7.3 Problem-Space Adversarial Attacks

Our experiments with physics-guided perturbations reveal a critical insight: the wireless propagation laws themselves impose a natural set of constraints that can be exploited as a defense surface. When perturbations are projected back into the physically realizable CSI manifold, most gradient-based attacks fail to preserve channel statistics or spectral-temporal consistency. This finding parallels results in other sensing domains – but in wireless sensing, such robustness can arise intrinsically from the physics rather than from architectural regularization or enforcing data consistency [10].

We therefore highlight the potential of combining *model-based* and *physics-based* robustness: training discriminators or priors that enforce energy, spectral, and spatial plausibility during both attack and defense. This direction opens pathways toward *certifiable robustness* rooted in physical signal realism, where propagation dynamics and channel coherence properties constrain adversarial perturbations. It is important to note that we assume our constraints serve as a filter for *problem-space attacks* in this domain [86].

7.4 Attacks in the Time Domain

A review of current open-source CSI datasets reveals several limitations: indoor-only capture, fixed transceiver pairs, limited scene diversity, and perfectly segmented samples. While convenient for training and reproducibility, these assumptions obscure important temporal vulnerabilities that arise in *continuous sensing* deployments. In dynamic, real-world environments, attackers could exploit temporal correlations to erode model confidence, inducing malicious *concept drift* that biases adaptive models over time. Future research should extend robustness evaluation beyond static adversarial examples to include long-term temporal attacks, adaptive drift injection, and online adversarial learning scenarios that better resemble real sensing systems.

7.5 Utility of a Modular Framework

The long-term value of this work lies in establishing a consistent, modular, and extensible benchmarking framework for adversarial robustness in wireless sensing. Analogous to how benchmarks such as ImageNet [87] or GLUE [88] catalyzed progress in vision and NLP robustness research, this benchmark lays the foundation for a reproducible platform for iterative advancement through the cycle of *attack* → *defense* → *re-evaluation*. Our open-source framework supports flexible integration of new CSI datasets, architectures, and defense mechanisms, enabling a common empirical basis.

Such a foundation is essential for fostering community-driven exploration of open questions – including cross-dataset transferability of attacks, multi-modal fusion robustness, and lightweight defensive retraining for edge devices – and to accelerate convergence toward trustworthy and certifiable wireless ML systems.

7.6 Limitations and Future Work

Our study presents three primary limitations. First, we evaluate only a single adversarial defense mechanism, namely projected gradient descent adversarial training (PGD-AT), which limits our understanding of how consistency-based or regularization-based defenses might alter the robustness-accuracy tradeoff. Second, the implemented pipelines currently target raw CSI datasets, and extending them to engineered representations such as BVP (Widar3.0) or Doppler-based features (SHARP) would yield a more complete robustness profile across signal hierarchies. Finally, the datasets used, though widely adopted in the community, remain small and controlled relative to real deployment settings. Expanding the benchmark to real-time, cross-device, and cross-environment sensing scenarios will be critical for evaluating practical reliability.

8 Conclusions

CSI-based sensing is poised to play a central role in future Wi-Fi systems, through standards such as IEEE 802.11bf, but its device-free and passive nature expands the attack surface. While most prior security research has focused on physical-layer manipulation, our study shows that the machine-learning layer remains an under-examined but crucial point of vulnerability. We argued that a strong and stealthy adversary will ultimately target the model’s decision-making process, and that evaluating robustness at this layer is essential for anticipating real-world risks.

To address this gap, we introduced a unified framework for evaluating adversarial robustness in CSI-based sensing and systematically compared model families, datasets, threat models, and physically realistic perturbations. We found that lightweight models, despite strong clean accuracy, are markedly more fragile; that transferability aligns with architectural similarity; and that physically constrained perturbations dramatically reduce attack success compared to unconstrained ones. A central insight that emerged is that robustness must leverage wireless propagation structure: enforcing spectral, temporal, and spatial realism nearly neutral-

lizes many attacks. Incorporating such constraints into model design, training, or detection, therefore, offers a promising path toward resilient CSI-based sensing. We release our modular framework to support reproducible robustness evaluation and to help guide the development of real, trustworthy wireless sensing systems.

Acknowledgments

Shreevanth Krishnaa Gopalakrishnan was supported by the EPSRC through the Centre for Doctoral Training Studentship in Cybersecurity (EP/S022503/1).

References

- [1] José Marcelo Fernandes et al. “A Survey of Approaches to Unobtrusive Sensing of Humans”. In: *ACM Computing Surveys* 55.2 (Feb. 28, 2023), pp. 1–28. ISSN: 0360-0300, 1557-7341. DOI: 10.1145/3491208. URL: <https://dl.acm.org/doi/10.1145/3491208> (visited on 08/09/2025).
- [2] Daniel Halperin et al. “Tool release: gathering 802.11n traces with channel state information”. In: *null* (2011). DOI: 10.1145/1925861.1925870.
- [3] Yaxiong Xie, Zhenjiang Li, and Mo Li. “Precise Power Delay Profiling with Commodity Wi-Fi”. In: *IEEE Transactions on Mobile Computing* 18.6 (June 2019), pp. 1342–1355. ISSN: 1558-0660. DOI: 10.1109/TMC.2018.2860991. URL: <https://ieeexplore.ieee.org/document/8423070> (visited on 11/11/2025).
- [4] Matthias Schulz, Daniel Wegemer, and Matthias Hollick. *Nexmon: The C-based Firmware Patching Framework*. 2017. URL: <https://nexmon.org>.
- [5] Steven M. Hernandez and Eyuphan Bulut. “Lightweight and Standalone IoT Based WiFi Sensing for Active Repositioning and Mobility”. In: *2020 IEEE 21st International Symposium on "A World of Wireless, Mobile and Multimedia Networks" (WoWMoM)*. 2020 IEEE 21st International Symposium on “A World of Wireless, Mobile and Multimedia Networks” (WoWMoM). Aug. 2020, pp. 277–286. DOI: 10.1109/WoWMoM49955.2020.00056. URL: <https://ieeexplore.ieee.org/document/9217780> (visited on 11/11/2025).
- [6] Zisheng Wang et al. *Wi-Fi Sensing Tool Release: Gathering 802.11ax Channel State Information from a Commercial Wi-Fi Access Point*. arXiv.org. June 20, 2025. URL: <https://arxiv.org/abs/2506.16957v1> (visited on 11/11/2025).
- [7] Ian J. Goodfellow, Jonathon Shlens, and Christian Szegedy. *Explaining and Harnessing Adversarial Examples*. GSAC: 0018260. Mar. 20, 2015. DOI: 10.48550/arXiv.1412.6572. arXiv: 1412.6572 [cs, stat]. URL: <http://arxiv.org/abs/1412.6572> (visited on 10/28/2022).

[8] Yuxuan Zhou et al. “WiAdv: Practical and Robust Adversarial Attack against WiFi-based Gesture Recognition System”. In: *Proceedings of the ACM on Interactive, Mobile, Wearable and Ubiquitous Technologies* 6.2 (July 4, 2022), pp. 1–25. ISSN: 2474-9567. DOI: 10.1145/3534618. URL: <https://dl.acm.org/doi/10.1145/3534618> (visited on 03/30/2025).

[9] Hangcheng Cao et al. *Security Analysis of WiFi-based Sensing Systems: Threats from Perturbation Attacks*. Apr. 24, 2024. arXiv: 2404.15587[cs]. URL: <http://arxiv.org/abs/2404.15587> (visited on 11/06/2024).

[10] Jianfei Yang, Han Zou, and Lihua Xie. “SecureSense: Defending Adversarial Attack for Secure Device-Free Human Activity Recognition”. In: *IEEE Transactions on Mobile Computing* 23.1 (Jan. 2024). Conference Name: IEEE Transactions on Mobile Computing, pp. 823–834. ISSN: 1558-0660. DOI: 10.1109/TMC.2022.3226742. URL: <https://ieeexplore.ieee.org/document/9972840/?arnumber=9972840> (visited on 04/01/2025).

[11] Iftikhar Ahmad, Arif Ullah, and Wooyeol Choi. “WiFi-Based Human Sensing With Deep Learning: Recent Advances, Challenges, and Opportunities”. In: *IEEE Open Journal of the Communications Society* 5 (2024), pp. 3595–3623. ISSN: 2644-125X. DOI: 10.1109/OJCOMS.2024.3411529. URL: <https://ieeexplore.ieee.org/document/10552143/> (visited on 08/09/2025).

[12] Yue Zheng et al. “Zero-Effort Cross-Domain Gesture Recognition with Wi-Fi”. In: *Proceedings of the 17th Annual International Conference on Mobile Systems, Applications, and Services*. MobiSys ’19. New York, NY, USA: Association for Computing Machinery, June 12, 2019, pp. 313–325. ISBN: 978-1-4503-6661-8. DOI: 10.1145/3307334.3326081. URL: <https://dl.acm.org/doi/10.1145/3307334.3326081> (visited on 04/14/2025).

[13] Ronghui Zhang et al. “Device-Free Wireless Sensing for Human Detection: The Deep Learning Perspective”. In: *IEEE Internet of Things Journal* 8.4 (Feb. 2021). GSCC: 0000141 2025-08-09T17:48:14.613Z 0.60, pp. 2517–2539. ISSN: 2327-4662. DOI: 10.1109/JIOT.2020.3024234. URL: <https://ieeexplore.ieee.org/document/9198891/> (visited on 06/06/2025).

[14] Sheng Tan et al. “Commodity WiFi Sensing in Ten Years: Status, Challenges, and Opportunities”. In: *IEEE Internet of Things Journal* 9.18 (Sept. 2022). GSCC: 0000143 2025-08-09T17:48:30.846Z 0.93, pp. 17832–17843. ISSN: 2327-4662. DOI: 10.1109/JIOT.2022.3164569. URL: <https://ieeexplore.ieee.org/document/9748867/> (visited on 06/06/2025).

[15] Isura Nirmal et al. “Deep Learning for Radio-Based Human Sensing: Recent Advances and Future Directions”. In: *IEEE Communications Surveys & Tutorials* 23.2 (2021). GSCC: 0000100 2025-08-09T17:48:32.108Z 0.41, pp. 995–1019. ISSN: 1553-877X. DOI: 10.1109/COMST.2021.3058333. URL: <https://ieeexplore.ieee.org/document/9353723/> (visited on 06/06/2025).

[16] Yongsen Ma, Gang Zhou, and Shuangquan Wang. “WiFi Sensing with Channel State Information: A Survey”. In: *ACM Computing Surveys* 52.3 (May 31, 2020), pp. 1–36. ISSN: 0360-0300, 1557-7341. DOI: 10.1145/3310194. URL: <https://dl.acm.org/doi/10.1145/3310194> (visited on 10/29/2024).

[17] Ruixu Geng et al. *A Survey of Wireless Sensing Security from a Role-Based View: Victim, Weapon, and Shield*. Dec. 4, 2024. DOI: 10.48550/arXiv.2412.03064. arXiv: 2412.03064[cs]. URL: <http://arxiv.org/abs/2412.03064> (visited on 12/09/2024).

[18] Chen Chen, Gang Zhou, and Youfang Lin. “Cross-Domain WiFi Sensing with Channel State Information: A Survey”. In: *ACM Computing Surveys* 55.11 (Nov. 30, 2023), pp. 1–37. ISSN: 0360-0300, 1557-7341. DOI: 10.1145/3570325. URL: <https://dl.acm.org/doi/10.1145/3570325> (visited on 10/29/2024).

[19] Tong Xin et al. “FreeSense: A Robust Approach for Indoor Human Detection Using Wi-Fi Signals”. In: *null* (2018). DOI: 10.1145/3264953.

[20] Lei Zhang et al. “Wi-Run: Multi-Runner Step Estimation Using Commodity Wi-Fi”. In: *null* (2018). DOI: 10.1109/sahcn.2018.8397122.

[21] Francesca Meneghelli et al. “SHARP: Environment and Person Independent Activity Recognition With Commodity IEEE 802.11 Access Points”. In: *IEEE Transactions on Mobile Computing* 22.10 (Oct. 2023). Conference Name: IEEE Transactions on Mobile Computing, pp. 6160–6175. ISSN: 1558-0660. DOI: 10.1109/TMC.2022.3185681. URL: <https://ieeexplore.ieee.org/document/9804861/?arnumber=9804861> (visited on 10/16/2024).

[22] Hao Wang et al. “RT-Fall: A Real-Time and Contactless Fall Detection System with Commodity WiFi Devices”. In: *IEEE Transactions on Mobile Computing* (2017). DOI: 10.1109/tmc.2016.2557795.

[23] Xuyu Wang et al. “PhaseBeat: Exploiting CSI Phase Data for Vital Sign Monitoring with Commodity WiFi Devices”. In: *null* (2017). DOI: 10.1109/icdcs.2017.206.

[24] Yongsen Ma et al. “SignFi: Sign Language Recognition Using WiFi”. In: *null* (2018). DOI: 10.1145/3191755.

[25] Linlin Guo et al. “Wiar: A Public Dataset for WiFi-Based Activity Recognition”. In: *IEEE Access* (2019). DOI: 10.1109/access.2019.2947024.

[26] Leiyang Xu et al. "WiCAM: Imperceptible Adversarial Attack on Deep Learning based WiFi Sensing". In: *2022 19th Annual IEEE International Conference on Sensing, Communication, and Networking (SECON)*. 2022 19th Annual IEEE International Conference on Sensing, Communication, and Networking (SECON). GSCC: 0000030 2025-09-06T18:33:55.318Z 0.19 ISSN: 2155-5494. Sept. 2022, pp. 10–18. DOI: 10.1109/SECON55815.2022.9918564. URL: <https://ieeexplore.ieee.org/document/9918564> (visited on 09/06/2025).

[27] Aryan Sharma et al. "Wi-Spoof: Generating adversarial wireless signals to deceive Wi-Fi sensing systems". In: *Journal of Information Security and Applications* 91 (June 1, 2025), p. 104052. ISSN: 2214-2126. DOI: 10.1016/j.jisa.2025.104052. URL: <https://www.sciencedirect.com/science/article/pii/S2214212625000894> (visited on 08/06/2025).

[28] Guolin Yin et al. "Evasion Attacks and Countermeasures in Deep Learning-Based Wi-Fi Gesture Recognition". In: *IEEE Transactions on Mobile Computing* 24.9 (Sept. 2025), pp. 8180–8195. ISSN: 1558-0660. DOI: 10.1109/TMC.2025.3557757. URL: <https://ieeexplore.ieee.org/document/10948311/> (visited on 09/22/2025).

[29] Siwang Zhou et al. "Adversarial WiFi Sensing for Privacy Preservation of Human Behaviors". In: *IEEE Communications Letters* 24.2 (Feb. 2020). Conference Name: IEEE Communications Letters, pp. 259–263. ISSN: 1558-2558. DOI: 10.1109/LCOMM.2019.2952844. URL: <https://ieeexplore.ieee.org/document/8897594> (visited on 03/24/2025).

[30] Wenda Li et al. "On CSI and Passive Wi-Fi Radar for Opportunistic Physical Activity Recognition". In: *IEEE Transactions on Wireless Communications* 21.1 (Jan. 2022). Conference Name: IEEE Transactions on Wireless Communications, pp. 607–620. ISSN: 1558-2248. DOI: 10.1109/TWC.2021.3098526. URL: <https://ieeexplore.ieee.org/document/9497736/?arnumber=9497736> (visited on 03/27/2025).

[31] Zheng Yang, Zimu Zhou, and Yunhao Liu. "From RSSI to CSI: Indoor localization via channel response". In: *ACM Computing Surveys* 46.2 (Nov. 2013). GSCC: 0001463 2025-08-09T17:48:22.165Z 0, pp. 1–32. ISSN: 0360-0300, 1557-7341. DOI: 10.1145/2543581.2543592. URL: <https://dl.acm.org/doi/10.1145/2543581.2543592> (visited on 06/09/2025).

[32] Rui Du et al. *An Overview on IEEE 802.11bf: WLAN Sensing*. Oct. 20, 2023. arXiv: 2310.17661. URL: <http://arxiv.org/abs/2310.17661> (visited on 11/08/2024).

[33] Cheng Chen et al. "Wi-Fi Sensing Based on IEEE 802.11bf". In: *IEEE Communications Magazine* 61.1 (Jan. 2023), pp. 121–127. ISSN: 0163-6804, 1558-1896. DOI: 10.1109/MCOM.007.2200347. URL: <https://ieeexplore.ieee.org/document/9941042/> (visited on 12/18/2024).

[34] Apostol Vassilev. *Adversarial Machine Learning: A Taxonomy and Terminology of Attacks and Mitigations*. NIST AI 100-2 E2025. Gaithersburg, MD: National Institute of Standards and Technology, 2025, NIST AI 100-2e2025. DOI: 10.6028/NIST.AI.100-2e2025. URL: <https://nvlpubs.nist.gov/nistpubs/ai/NIST.AI.100-2e2025.pdf> (visited on 09/22/2025).

[35] Nikolaos Pitropakis et al. "A taxonomy and survey of attacks against machine learning". In: *Computer Science Review* 34 (Nov. 2019). GSCC: 0000239, p. 100199. ISSN: 15740137. DOI: 10.1016/j.cosrev.2019.100199. URL: <https://linkinghub.elsevier.com/retrieve/pii/S1574013718303289> (visited on 11/27/2023).

[36] Aleksander Madry et al. "Towards Deep Learning Models Resistant to Adversarial Attacks". In: International Conference on Learning Representations. GSCC: 0010212. Feb. 15, 2018. URL: <https://openreview.net/forum?id=rJzIBfZAb> (visited on 12/02/2023).

[37] Jihoon Tack et al. *Consistency Regularization for Adversarial Robustness*. Dec. 23, 2021. DOI: 10.48550/arXiv.2103.04623. arXiv: 2103.04623[cs]. URL: <http://arxiv.org/abs/2103.04623> (visited on 11/11/2025).

[38] Chuan Guo et al. *Countering Adversarial Images using Input Transformations*. Jan. 29, 2018. DOI: 10.48550/arXiv.1711.00117. arXiv: 1711.00117[cs]. URL: <http://arxiv.org/abs/1711.00117> (visited on 11/11/2025).

[39] Cheng Zhang and Pan Gao. *Countering Adversarial Examples: Combining Input Transformation and Noisy Training*. June 28, 2021. DOI: 10.48550/arXiv.2106.13394. arXiv: 2106.13394[cs]. URL: <http://arxiv.org/abs/2106.13394> (visited on 11/11/2025).

[40] Eric Wong and J. Zico Kolter. *Provable defenses against adversarial examples via the convex outer adversarial polytope*. GSCC: 0001498. June 8, 2018. DOI: 10.48550/arXiv.1711.00851. arXiv: 1711.00851[cs, math]. URL: <http://arxiv.org/abs/1711.00851> (visited on 12/02/2023).

[41] Jeremy Cohen, Elan Rosenfeld, and Zico Kolter. "Certified Adversarial Robustness via Randomized Smoothing". In: *Proceedings of the 36th International Conference on Machine Learning*. International Conference on Machine Learning. GSCC: 0001662 ISSN: 2640-3498. PMLR, May 24, 2019, pp. 1310–1320. URL: <https://proceedings.mlr.press/v97/cohen20a.html> (visited on 11/08/2024).

mlr.press/v97/cohen19c.html (visited on 12/02/2023).

[42] Jiahao Wang et al. “Transfer Learning for Indoor Localization Algorithm Based on Deep Domain Adaptation”. In: *Sensors* 23.23 (Jan. 2023). Publisher: Multidisciplinary Digital Publishing Institute, p. 9334. ISSN: 1424-8220. DOI: 10.3390/s23239334. URL: <https://www.mdpi.com/1424-8220/23/23/9334> (visited on 11/12/2025).

[43] Xinyi Li et al. “Towards Collaborative and Cross-Domain Wi-Fi Sensing: A Case Study for Human Activity Recognition”. In: *IEEE Transactions on Mobile Computing* 23.2 (Feb. 2024), pp. 1674-1688. ISSN: 1558-0660. DOI: 10.1109/TMC.2023.3242324. URL: <https://ieeexplore.ieee.org/document/10036978> (visited on 11/12/2025).

[44] Guolin Yin et al. *FewSense, Towards a Scalable and Cross-Domain Wi-Fi Sensing System Using Few-Shot Learning*. Mar. 7, 2022. DOI: 10.48550/arXiv.2203.02014. arXiv: 2203.02014[eess]. URL: <http://arxiv.org/abs/2203.02014> (visited on 11/12/2025).

[45] Zhengjie Wang et al. “Review of few-shot learning application in CSI human sensing”. In: *Artificial Intelligence Review* 57.8 (July 5, 2024), p. 195. ISSN: 1573-7462. DOI: 10.1007/s10462-024-10812-4. URL: <https://doi.org/10.1007/s10462-024-10812-4> (visited on 11/12/2025).

[46] Zijian Zhao et al. “CrossFi: A Cross Domain Wi-Fi Sensing Framework Based on Siamese Network”. In: *IEEE Internet of Things Journal* 12.12 (June 15, 2025), pp. 20138-20155. ISSN: 2327-4662, 2372-2541. DOI: 10.1109/JIOT.2025.3542850. arXiv: 2408.10919[cs]. URL: <http://arxiv.org/abs/2408.10919> (visited on 11/12/2025).

[47] Dazhuo Wang et al. “AirFi: Empowering WiFi-Based Passive Human Gesture Recognition to Unseen Environment via Domain Generalization”. In: *IEEE Transactions on Mobile Computing* 23.2 (Feb. 1, 2024), pp. 1156-1168. ISSN: 1536-1233. DOI: 10.1109/TMC.2022.3230665. URL: <https://doi.org/10.1109/TMC.2022.3230665> (visited on 11/12/2025).

[48] Dingzhu Wen et al. *Integrated Sensing, Communication, and Computation for Over-the-Air Federated Edge Learning*. Aug. 22, 2025. DOI: 10.48550/arXiv.2508.15185. arXiv: 2508.15185[cs]. URL: <http://arxiv.org/abs/2508.15185> (visited on 11/12/2025).

[49] Yo-Seb Jeon et al. “A Compressive Sensing Approach for Federated Learning Over Massive MIMO Communication Systems”. In: *IEEE Transactions on Wireless Communications* 20.3 (Mar. 2021), pp. 1990-2004. ISSN: 1536-1276, 1558-2248. DOI: 10.1109/TWC.2020.3038407. URL: <https://ieeexplore.ieee.org/document/9269459/> (visited on 11/12/2025).

[50] Montaser N. A. Ramadan et al. “Federated learning and TinyML on IoT edge devices: Challenges, advances, and future directions”. In: *ICT Express* 11.4 (Aug. 2025). Publisher: Korean Institute of Communications and Information Sciences, pp. 754-768. DOI: 10.1016/j.ictexpress.2025.06.008. URL: <https://nchr.elsevierpure.com/en/publications/federated-learning-and-tinyml-on-iot-edge-devices-challenges-adva/> (visited on 11/12/2025).

[51] Wei Sun, Tingjun Chen, and Neil Gong. “SoK: Secure Human-centered Wireless Sensing”. In: *Proceedings on Privacy Enhancing Technologies* 2024.2 (Apr. 2024), pp. 313-329. ISSN: 2299-0984. DOI: 10.56553/popets-2024-0052. URL: <https://petsymposium.org/popets/2024/popets-2024-0052.php> (visited on 10/16/2024).

[52] Mengyuan Li et al. “When CSI Meets Public WiFi: Inferring Your Mobile Phone Password via WiFi Signals”. In: *Proceedings of the 2016 ACM SIGSAC Conference on Computer and Communications Security*. CCS ’16. New York, NY, USA: Association for Computing Machinery, Oct. 24, 2016, pp. 1068-1079. ISBN: 978-1-4503-4139-4. DOI: 10.1145/2976749.2978397. URL: <https://dl.acm.org/doi/10.1145/2976749.2978397> (visited on 11/11/2025).

[53] Pengsong Duan et al. “A Comprehensive Survey on Wi-Fi Sensing for Human Identity Recognition”. In: *Electronics* 12.23 (Jan. 2023). Publisher: Multidisciplinary Digital Publishing Institute, p. 4858. ISSN: 2079-9292. DOI: 10.3390/electronics12234858. URL: <https://www.mdpi.com/2079-9292/12/23/4858> (visited on 11/12/2025).

[54] Yu Gu et al. “WiGRUNT: WiFi-Enabled Gesture Recognition Using Dual-Attention Network”. In: *IEEE Transactions on Human-Machine Systems* 52.4 (Aug. 2022), pp. 736-746. ISSN: 2168-2305. DOI: 10.1109/THMS.2022.3163189. URL: <https://ieeexplore.ieee.org/document/9759238/> (visited on 06/06/2025).

[55] Yanzi Zhu et al. “Et Tu Alexa? When Commodity WiFi Devices Turn into Adversarial Motion Sensors”. In: *Proceedings 2020 Network and Distributed System Security Symposium*. Network and Distributed System Security Symposium. San Diego, CA: Internet Society, 2020. ISBN: 978-1-891562-61-7. DOI: 10.14722/ndss.2020.23053. URL: <https://www.ndss-symposium.org/wp-content/uploads/2020/02/23053.pdf> (visited on 03/24/2025).

[56] Tanguy Ropital et al. “Overhead-Free People Counting in mmWave Networks Using IEEE 802.11bf Passive Sensing”. In: *2024 IEEE 35th International Symposium on Personal, Indoor and Mobile Radio Communications (PIMRC)*. 2024 IEEE 35th International Symposium on Personal, Indoor

and Mobile Radio Communications (PIMRC). ISSN: 2166-9589. Sept. 2024, pp. 1–6. DOI: 10.1109/PIMRC59610.2024.10817454. URL: <https://ieeexplore.ieee.org/document/10817454> (visited on 11/12/2025).

[57] Jianfei Yang et al. “Device-Free Occupant Activity Sensing Using WiFi-Enabled IoT Devices for Smart Homes”. In: *IEEE Internet of Things Journal* 5.5 (Oct. 2018), pp. 3991–4002. ISSN: 2327-4662. DOI: 10.1109/JIOT.2018.2849655. URL: <https://ieeexplore.ieee.org/document/8391737> (visited on 11/12/2025).

[58] Fei Wang et al. “WiPIN: Operation-Free Passive Person Identification Using Wi-Fi Signals”. In: *2019 IEEE Global Communications Conference (GLOBECOM)*. GLOBECOM 2019 - 2019 IEEE Global Communications Conference. Waikoloa, HI, USA: IEEE, Dec. 2019, pp. 1–6. ISBN: 978-1-7281-0962-6. DOI: 10.1109/GLOBECOM38437.2019.9014226. URL: <https://ieeexplore.ieee.org/document/9014226/> (visited on 11/12/2025).

[59] Tong Xin et al. “FreeSense: Indoor Human Identification with Wi-Fi Signals”. In: *2016 IEEE Global Communications Conference (GLOBECOM)*. Washington, DC, USA: IEEE Press, Dec. 4, 2016, pp. 1–7. DOI: 10.1109/GLOCOM.2016.7841847. URL: <https://doi.org/10.1109/GLOCOM.2016.7841847> (visited on 11/11/2025).

[60] Yue Qiao et al. “PhyCloak: obfuscating sensing from communication signals”. In: *Proceedings of the 13th Usenix Conference on Networked Systems Design and Implementation*. NSDI’16. USA: USENIX Association, Mar. 16, 2016, pp. 685–699. ISBN: 978-1-931971-29-4. (Visited on 11/11/2025).

[61] Antonios Argyriou. “Obfuscation of Human Micro-Doppler Signatures in Passive Wireless RADAR”. In: *IEEE Access* 11 (2023), pp. 40121–40127. ISSN: 2169-3536. DOI: 10.1109/ACCESS.2023.3269435. arXiv: 2303.03001[cs, eess]. URL: <http://arxiv.org/abs/2303.03001> (visited on 06/20/2024).

[62] Yao Yao et al. “Aegis: An Interference-Negligible RF Sensing Shield”. In: *IEEE INFOCOM 2018 - IEEE Conference on Computer Communications*. IEEE INFOCOM 2018 - IEEE Conference on Computer Communications. Apr. 2018, pp. 1718–1726. DOI: 10.1109/INFOCOM.2018.8485883. URL: <https://ieeexplore.ieee.org/document/8485883> (visited on 06/20/2024).

[63] Fei Xiao et al. “Over-the-Air Adversarial Attacks on Deep Learning Wi-Fi Fingerprinting”. In: *IEEE Internet of Things Journal* 10.11 (June 2023), pp. 9823–9835. ISSN: 2327-4662. DOI: 10.1109/JIOT.2023.3236314. URL: <https://ieeexplore.ieee.org/document/10015738> (visited on 11/12/2025).

[64] Changming Li et al. “Practical Adversarial Attack on WiFi Sensing Through Unnoticeable Communication Packet Perturbation”. In: *Proceedings of the 30th Annual International Conference on Mobile Computing and Networking*. ACM MobiCom ’24: 30th Annual International Conference on Mobile Computing and Networking. Washington D.C. DC USA: ACM, May 29, 2024, pp. 373–387. ISBN: 978-8-4007-0489-5. DOI: 10.1145/3636534.3649367. URL: <https://dl.acm.org/doi/10.1145/3636534.3649367> (visited on 11/06/2024).

[65] Zikun Liu et al. “Exploring Practical Vulnerabilities of Machine Learning-based Wireless Systems”. In: *20th USENIX Symposium on Networked Systems Design and Implementation (NSDI 23)*. Boston, MA: USENIX Association, Apr. 2023, pp. 1801–1817. ISBN: 978-1-939133-33-5. URL: <https://www.usenix.org/conference/nsdi23/presentation/liu-zikun>.

[66] Brian Kim et al. “Channel-Aware Adversarial Attacks Against Deep Learning-Based Wireless Signal Classifiers”. In: *IEEE Transactions on Wireless Communications* 21.6 (June 2022), pp. 3868–3880. ISSN: 1558-2248. DOI: 10.1109/TWC.2021.3124855. URL: <https://ieeexplore.ieee.org/document/9609969/> (visited on 11/12/2025).

[67] Nicholas Carlini and David Wagner. *Towards Evaluating the Robustness of Neural Networks*. Mar. 23, 2017. DOI: 10.48550/arXiv.1608.04644. arXiv: 1608.04644[cs]. URL: <http://arxiv.org/abs/1608.04644> (visited on 11/12/2025).

[68] Giulio Zizzo et al. “Adversarial Attacks on Time-Series Intrusion Detection for Industrial Control Systems”. In: *2020 IEEE 19th International Conference on Trust, Security and Privacy in Computing and Communications (TrustCom)*. 2020 IEEE 19th International Conference on Trust, Security and Privacy in Computing and Communications (TrustCom). Guangzhou, China: IEEE, Dec. 2020, pp. 899–910. ISBN: 978-1-6654-0392-4. DOI: 10.1109/TrustCom50675.2020.00121. URL: <https://ieeexplore.ieee.org/document/9343061/> (visited on 10/04/2022).

[69] Gautier Pialla et al. “Time series adversarial attacks: an investigation of smooth perturbations and defense approaches”. In: *International Journal of Data Science and Analytics* 19.1 (Jan. 1, 2025), pp. 129–139. ISSN: 2364-4168. DOI: 10.1007/s41060-023-00438-0. URL: <https://doi.org/10.1007/s41060-023-00438-0> (visited on 02/14/2025).

[70] Harshit Ambalkar, Xuyu Wang, and Shiwen Mao. “Adversarial Human Activity Recognition Using WiFi CSI”. In: *2021 IEEE Canadian Conference on Electrical and Computer Engineering (CCECE)*. 2021 IEEE Canadian Conference on Electrical and Computer Engineering (CCECE). ISSN: 2576-7046. Sept. 2021, pp. 1–5. DOI: 10.1109/CCECE53047.2021.9569098. URL: <https://ieeexplore.ieee.org/document/9569098>.

/ / ieeexplore . ieee . org / document / 9569098 / ?arnumber = 9569098 (visited on 12/09/2024).

[71] Sungkwan Youm and Sunghyun Go. “Lightweight and Efficient CSI-Based Human Activity Recognition via Bayesian Optimization-Guided Architecture Search and Structured Pruning”. In: *Applied Sciences* 15.2 (Jan. 2025). Publisher: Multidisciplinary Digital Publishing Institute, p. 890. ISSN: 2076-3417. DOI: 10 . 3390 / app15020890. URL: <https://www.mdpi.com/2076-3417/15/2/890> (visited on 11/12/2025).

[72] Hojjat Salehinejad and Shahrokh Valaee. *LiteHAR: Lightweight Human Activity Recognition from WiFi Signals with Random Convolution Kernels*. arXiv.org. Jan. 23, 2022. DOI: 10 . 1109 / ICASSP43922 . 2022 . 9746803. URL: <https://arxiv.org/abs/2201.09310v1> (visited on 11/12/2025).

[73] Chuan Liu et al. “LiteWiHAR: A Lightweight WiFi-based Human Activity Recognition System”. In: *2024 IEEE 99th Vehicular Technology Conference (VTC2024-Spring)*. 2024 IEEE 99th Vehicular Technology Conference (VTC2024-Spring). Singapore, Singapore: IEEE, June 24, 2024, pp. 1–5. ISBN: 979-8-3503-8741-4. DOI: 10 . 1109 / VTC2024 - Spring62846 . 2024 . 10683210. URL: <https://ieeexplore.ieee.org/document/10683210/> (visited on 11/12/2025).

[74] Sarab AlMuhaideb et al. “Achieving More with Less: A Lightweight Deep Learning Solution for Advanced Human Activity Recognition (HAR)”. In: *Sensors* 24.16 (Jan. 2024). Publisher: Multidisciplinary Digital Publishing Institute, p. 5436. ISSN: 1424-8220. DOI: 10 . 3390 / s24165436. URL: <https://www.mdpi.com/1424-8220/24/16/5436> (visited on 11/12/2025).

[75] Jianfei Yang et al. “EfficientFi: Toward Large-Scale Lightweight WiFi Sensing via CSI Compression”. In: *IEEE Internet of Things Journal* 9.15 (Aug. 2022), pp. 13086–13095. ISSN: 2327-4662. DOI: 10 . 1109 / JIOT . 2021 . 3139958. URL: <https://ieeexplore.ieee.org/document/9667414/> (visited on 04/14/2025).

[76] Jianfei Yang et al. *SenseFi: A Library and Benchmark on Deep-Learning-Empowered WiFi Human Sensing*. Feb. 17, 2023. arXiv: 2207 . 07859. URL: <http://arxiv.org/abs/2207.07859> (visited on 11/08/2024).

[77] Siamak Yousefi et al. “A Survey on Behavior Recognition Using WiFi Channel State Information”. In: *IEEE Communications Magazine* 55.10 (Oct. 2017). GSAC: 0000601 2025-08-09T17:48:16.478Z 1.47, pp. 98–104. ISSN: 1558-1896. DOI: 10 . 1109 / MCOM . 2017 . 1700082. URL: <https://ieeexplore.ieee.org/document/8067693/> (visited on 06/06/2025).

[78] Dazhuo Wang et al. “CAUTION: A Robust WiFi-Based Human Authentication System via Few-Shot Open-Set Recognition”. In: *IEEE Internet of Things Journal* 9.18 (Sept. 2022), pp. 17323–17333. ISSN: 2327-4662. DOI: 10 . 1109 / JIOT . 2022 . 3156099. URL: <https://ieeexplore.ieee.org/document/9726794> (visited on 11/12/2025).

[79] Seyed-Mohsen Moosavi-Dezfooli, Alhussein Fawzi, and Pascal Frossard. *DeepFool: a simple and accurate method to fool deep neural networks*. July 4, 2016. DOI: 10 . 48550 / arXiv . 1511 . 04599. arXiv: 1511 . 04599[cs]. URL: <http://arxiv.org/abs/1511.04599> (visited on 09/17/2025).

[80] Seyed-Mohsen Moosavi-Dezfooli et al. *Universal adversarial perturbations*. Mar. 9, 2017. DOI: 10 . 48550 / arXiv . 1610 . 08401. arXiv: 1610 . 08401[cs]. URL: <http://arxiv.org/abs/1610.08401> (visited on 09/17/2025).

[81] David Tse and Pramod Viswanath. *Fundamentals of wireless communication*. Cambridge: Cambridge University Press, 2005. 1 p. ISBN: 978-0-521-84527-4. DOI: 10 . 1017 / CBO9780511807213.

[82] Cheng-Xiang Wang et al. “Spatial-Temporal Correlation Properties of the 3GPP Spatial Channel Model and the Kronecker MIMO Channel Model”. In: *EURASIP Journal on Wireless Communications and Networking* 2007.1 (Dec. 2007). Publisher: SpringerOpen, pp. 1–9. ISSN: 1687-1499. DOI: 10 . 1155 / 2007 / 39871. URL: <https://jwcn-eurasipjournals.springeropen.com/articles/10.1155/2007/39871> (visited on 11/12/2025).

[83] Arthur Gretton et al. “A kernel two-sample test”. In: *J. Mach. Learn. Res.* 13 (null Mar. 1, 2012), pp. 723–773. ISSN: 1532-4435.

[84] Yuh-Shyan Chen, Chun-Yu Li, and Tong-Ying Juang. “Dynamic Associate Domain Adaptation for Human Activity Recognition Using WiFi Signals”. In: *2022 IEEE Wireless Communications and Networking Conference (WCNC)*. 2022 IEEE Wireless Communications and Networking Conference (WCNC). Austin, TX, USA: IEEE, Apr. 10, 2022, pp. 1809–1814. ISBN: 978-1-6654-4266-4. DOI: 10 . 1109 / WCNC51071 . 2022 . 9771677. URL: <https://ieeexplore.ieee.org/document/9771677/> (visited on 11/12/2025).

[85] Zijian Zhao et al. *KNN-MMD: Cross Domain Wireless Sensing via Local Distribution Alignment*. arXiv.org. Dec. 6, 2024. URL: <https://arxiv.org/abs/2412.04783v4> (visited on 11/12/2025).

[86] Fabio Pierazzi et al. “Intriguing Properties of Adversarial ML Attacks in the Problem Space”. In: *2020 IEEE Symposium on Security and Privacy (SP)*. 2020, pp. 1332–1349. DOI: 10 . 1109 / SP40000 . 2020 . 00073.

- [87] Jia Deng et al. “ImageNet: A large-scale hierarchical image database”. In: *2009 IEEE Conference on Computer Vision and Pattern Recognition*. 2009, pp. 248–255. DOI: 10.1109/CVPR.2009.5206848.
- [88] Alex Wang et al. *GLUE: A Multi-Task Benchmark and Analysis Platform for Natural Language Understanding*. 2019. arXiv: 1804 . 07461 [cs.CL]. URL: <https://arxiv.org/abs/1804.07461>.